

Negative Excess Shot Noise by Anyon Braiding

Byeongmok Lee, Cheolhee Han, and H.-S. Sim*

Department of Physics, Korea Advanced Institute of Science and Technology, Daejeon 34141, Korea

(Dated: December 4, 2021)

Anyonic fractional charges e^* have been detected by autocorrelation shot noise at a quantum point contact (QPC) between two fractional quantum Hall edges. We find that the autocorrelation noise can also show a fingerprint of Abelian anyonic fractional statistics. We predict the noise of electrical tunneling current I at the QPC of the fractional-charge detection setup, when anyons are dilutely injected, from an additional edge biased by a voltage, to the setup in equilibrium. At large voltages, the nonequilibrium noise is *reduced* below the thermal equilibrium noise by the value $2e^*I$. This negative excess noise is opposite to the positive excess noise $2e^*I$ of the conventional fractional-charge detection and also to usual positive autocorrelation noises of electrical currents. This is a signature of the Abelian fractional statistics, resulting from the effective braiding of an anyon thermally excited at the QPC around another anyon injected from the additional edge.

Abelian anyons appear in fractional quantum Hall (FQH) systems of filling factor $\nu = 1/(2n + 1)$, $n = 1, 2, \dots$. They obey the fractional exchange statistics [1–3]. Two anyons gain the phase $\pm\pi\nu$ when their positions are adiabatically exchanged, and $\pm 2\pi\nu$ when one braids around the other. Proposals [4–20] for detecting the fractional statistics are based on interferometers or current-current cross-correlations. They involve quantities experimentally inaccessible or affected by unintended setup change or Coulomb interaction. It will be useful to find fractional-statistics effects experimentally feasible.

Shot noise S , zero-frequency nonequilibrium fluctuation of electrical current I , has valuable information [21]. Its Poisson value $S = 2qI$ in the tunneling regime of a quantum point contact (QPC) was used to detect the charge q of current carriers [22]. The fractional charge $e^* = \nu e$ of anyons was measured [23–29] from the ratio $S/I = 2e^*$ at a QPC between FQH edges; e is the electron charge. The Poisson value originates from uncorrelated transfer of discrete charges. Reduction or enhancement from the value signifies effects such as resonances, diffusive scattering, Cooper pairing, etc [21].

In this work, we predict unusual behavior of shot noise, originating from the Abelian fractional statistics of Laughlin anyons, in the setup [Fig. 1(a)] composed of the conventional fractional-charge detection part (Edge2, Edge3, QPC2) and an additional edge (Edge1). Anyons are dilutely injected [30–33] via QPC1 from Edge1, biased by voltage V , to the detection part in equilibrium. We find that the zero-frequency autocorrelation noise $S(V, T)$ of tunneling current I at QPC2 is *reduced* below the thermal equilibrium noise $S(0, T)$ at temperature T ,

$$\delta S = -2e^*I < 0 \quad \text{at} \quad e^*V \gg k_B T. \quad (1)$$

$\delta S \equiv S(V, T) - S(0, T)$ is the excess shot noise with respect to the thermal noise and k_B is Boltzmann constant. The negative excess noise is unusual, since the setup has the conventional Poisson process [Fig. 1(b)] enhancing the noise; it is opposite to the positive noise $2e^*I > 0$ of the conventional fractional-charge detec-

tion [23–29]. By contrast, in the integer quantum Hall regime at $\nu = 1$, the setup shows the positive Poisson noise of $\delta S = 2eI > 0$, which cannot be extrapolated from Eq. (1) with $e^* = e/(2n + 1) \rightarrow e$.

The negative excess noise results from an interference involving anyon braiding [Fig. 1(c)], which weakens thermal anyon tunneling at QPC2, reducing the noise. The reduction dominates over the enhancement by the Poisson process. Interestingly, for electrons at $\nu = 1$, the interference does not exist, as it is described by a pair of disconnected Feynman diagrams that exactly cancel each other, according to the linked cluster theorem [34]. For anyons, the cancellation is only partial, since the subdia-

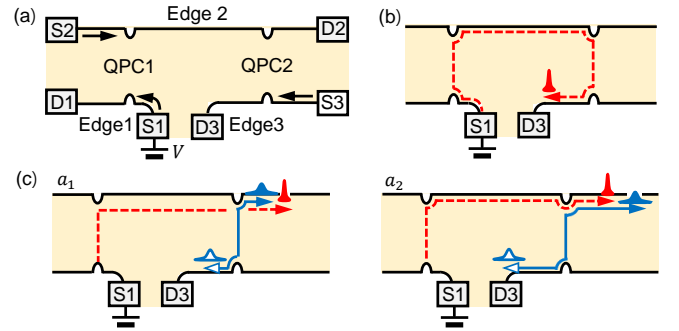


FIG. 1. (a) Setup at $\nu = \frac{1}{2n+1}$. Chiral edge channel Edge i propagates (arrows) from source S_i to drain D_i , $i = 1, 2, 3$. S_1 is biased by voltage V , while the other sources and drains are grounded. Anyon tunneling occurs at QPC1 (QPC2) between Edge2 and Edge1 (Edge3). (b) Poisson process. A particle-like anyon biased by V (narrow filled packets, dashed arrows) moves from Edge1 to D3 through tunneling at QPC1 and QPC2. (c) Interference between subprocesses a_1 and a_2 . A particle-like anyon biased by V moves (dashed) from Edge1 to D2 through tunneling at QPC1. After (before) this anyon passes QPC2 along Edge2, a particle-hole pair excitation thermally occurs at QPC2 in a_1 (a_2). The particle-like anyon (wide filled packets) and the hole-like anyon (wide empty) in the pair move (solid arrows) along Edge2 and Edge3, respectively. The interference between a_1 and a_2 involves braiding of the thermal anyon around the voltage-biased anyon.

grams (vacuum bubbles) of one of the disconnected diagrams are linked [35] by the braiding. This type of anyon processes, vacuum bubbles linked by braiding, is called topological vacuum bubbles (TVBs) [36]. Detection of the negative excess noise is experimentally feasible, and will provide a signature of TVBs and the fractional statistics in the case of pristine edges (without edge reconstruction). The signature manifests itself in the leading-order contributions (in QPC tunneling strengths) to the excess noise, thanks to the dilute anyon injection at QPC1.

Excess noise.— We consider the time t average $I = \overline{I(t)}$ of tunneling current $I(t)$ at QPC2, and its zero-frequency noise $S = 2 \int_{-\infty}^{\infty} dt (I(t) - I)(I(0) - I)$. Employing a perturbation theory based on the chiral Luttinger liquid [37, 38], Keldysh Green's functions, and Klein factors [39], we derive I and $\delta S = S(V, T) - S(0, T)$ at voltages $e^*V \gg k_B T$ in the anyon tunneling regime of $\gamma_i T^{\nu-1} \ll 1$, up to the leading order $O(\gamma_1^2 \gamma_2^2)$ of tunneling strength γ_i at QPC*i*,

$$I \simeq e^* \gamma_1^2 \gamma_2^2 f(\nu) [\cos(\pi\nu) - \cos(3\pi\nu)] V^{2\nu-1} T^{2\nu-2}, \quad (2)$$

$$\delta S \simeq -2e^* \gamma_1^2 \gamma_2^2 f(\nu) [\cos(\pi\nu) - \cos(3\pi\nu)] V^{2\nu-1} T^{2\nu-2}.$$

This gives Eq. (1) [40, 41]. Notice that $I > 0$ but $\delta S < 0$. The factors having $\pi\nu$ originate from anyon braiding.

The current I and excess noise δS are linked to measurable quantities. I equals the average current $I_3 = \overline{I_3(t)}$ at D3, as only S1 is biased. δS is obtained [41] by

$$\delta S = S_3(V, T) - 4k_B T \left. \frac{\partial I_3(V, T, V_3)}{\partial V_3} \right|_{V_3=0} - \left[S_3(0, T) - 4k_B T \left. \frac{\partial I_3(0, T, V_3)}{\partial V_3} \right|_{V_3=0} \right]. \quad (3)$$

The noise $S_3(V, T) = 2 \int_{-\infty}^{\infty} dt (I_3(t) - I_3)(I_3(0) - I_3)$ is measured at D3. $\partial I_3(V, T, V_3)/\partial V_3|_{V_3=0}$ is measured with the voltage V_3 applied to S3 in addition to the voltage V at S1, and equals the correlation between the tunneling current $I(t)$ at QPC2 and the current from S3 to QPC2, according to the nonequilibrium fluctuation-dissipation theorem [42–44].

Main processes.— We discuss the origin of $\delta S < 0$. The tunneling current and its excess noise satisfy [45] $I = e^*(W_{2 \rightarrow 3} - W_{3 \rightarrow 2})$ and $\delta S = 2(e^*)^2(W_{2 \rightarrow 3} + W_{3 \rightarrow 2})$. $W_{2 \rightarrow 3}$ ($W_{3 \rightarrow 2}$) is the change, by the voltage V , in the rate for a particle-like (hole-like) anyon to move from Edge2 to Edge3 at QPC2. Two types of processes, Poisson processes and TVBs, make contribution $W_{i \rightarrow j}^P$ and $W_{i \rightarrow j}^{\text{TVB}}$, respectively, to $W_{i \rightarrow j}$,

$$W_{i \rightarrow j} \simeq W_{i \rightarrow j}^P + W_{i \rightarrow j}^{\text{TVB}} \quad \text{at } e^*V \gg k_B T. \quad (4)$$

$W_{i \rightarrow j}$ is computed in Ref. [41].

In the Poisson process [Fig. 1(b)] for $W_{2 \rightarrow 3}^P$, a particle-like anyon, biased by the voltage V , moves from Edge1 to Edge3 through tunneling at QPC1 and QPC2. This leads

to $W_{2 \rightarrow 3}^P \propto \gamma_1^2 \gamma_2^2 V^{4\nu-3}$, as the voltage-biased tunneling probability at QPC*i* and the current from S1 to QPC1 are proportional to $\gamma_i^2 V^{2\nu-2}$ and V , respectively. By contrast, $W_{3 \rightarrow 2}^P = 0$, since tunneling of a hole-like anyon from Edge2 to Edge3 is not induced by V .

Next, we consider the TVB for $W_{3 \rightarrow 2}^{\text{TVB}}$. It is the interference of two subprocesses a_1 and a_2 [Fig. 1(c)]. In a_1 and a_2 , a particle-like anyon, induced by the voltage V , moves from Edge1 to Edge2 via tunneling at QPC1 at time t_1 , and then moves to D2. The operator for the QPC1 tunneling is $\mathcal{T}_{1 \rightarrow 2}(t_1) = \Psi_2^\dagger(0, t_1) \Psi_1(0, t_1)$. $\Psi_i^\dagger(x_i, t_1)$ creates an anyon at position x_i of Edge*i*; QPC1 is located at $x_i = 0$. After (before) this anyon passes QPC2, a particle-hole pair is thermally excited at QPC2 at time t_2 (t'_2) in the subprocess a_1 (a_2). Then the particle-like thermal anyon moves to D2 along Edge2, while the hole-like one to D3 along Edge3. The excitation is described by the QPC2 tunneling operator $\mathcal{T}_{3 \rightarrow 2}(t) = \Psi_2^\dagger(d, t) \Psi_3(0, t)$ at $t = t_2$ (t'_2) in a_1 (a_2); QPC2 is located at $x_2 = d$ ($x_3 = 0$) on Edge2 (Edge3).

To illustrate the nontrivial features (topological link by anyon braiding and the partner disconnected process) of the TVB for $W_{3 \rightarrow 2}^{\text{TVB}}$, we consider the $V \rightarrow \infty$ limit where the voltage-biased particle-like anyon becomes a point particle (its spatial broadening $\hbar v/(e^*V) \rightarrow 0$; v is the anyon velocity). In this limit, the correlator

$$C_{3 \rightarrow 2}^{\text{TVB}} = \langle \mathcal{T}_{1 \rightarrow 2}^\dagger(t_1) \mathcal{T}_{3 \rightarrow 2}^\dagger(t'_2) \mathcal{T}_{3 \rightarrow 2}(t_2) \mathcal{T}_{1 \rightarrow 2}(t_1) \rangle - \langle \mathcal{T}_{3 \rightarrow 2}^\dagger(t'_2) \mathcal{T}_{3 \rightarrow 2}(t_2) \rangle \langle \mathcal{T}_{1 \rightarrow 2}^\dagger(t_1) \mathcal{T}_{1 \rightarrow 2}(t_1) \rangle \quad (5)$$

describes the TVB. $\langle \dots \rangle$ is the ensemble average with the bare Hamiltonian [41] H_i of Edge*i*.

The first term of Eq. (5) shows the interference between the subprocesses a_1 and a_2 ; $\mathcal{T}_{3 \rightarrow 2}(t_2) \mathcal{T}_{1 \rightarrow 2}(t_1)$ describes a_1 , while $\mathcal{T}_{3 \rightarrow 2}(t'_2) \mathcal{T}_{1 \rightarrow 2}(t_1)$ describes a_2 . This term is factorized [41] into a subcorrelator for the voltage-biased anyon, another for the thermal anyons, and a phase factor $e^{i2\pi\nu}$ (Fig. 2),

$$\langle \mathcal{T}_{1 \rightarrow 2}^\dagger(t_1) \mathcal{T}_{3 \rightarrow 2}^\dagger(t'_2) \mathcal{T}_{3 \rightarrow 2}(t_2) \mathcal{T}_{1 \rightarrow 2}(t_1) \rangle = e^{i2\pi\nu} \langle \mathcal{T}_{3 \rightarrow 2}^\dagger(t'_2) \mathcal{T}_{3 \rightarrow 2}(t_2) \rangle \langle \mathcal{T}_{1 \rightarrow 2}^\dagger(t_1) \mathcal{T}_{1 \rightarrow 2}(t_1) \rangle, \quad (6)$$

by using the exchange rules of the fractional statistics $\Psi_i^\dagger(x) \Psi_i(y) = \Psi_i(y) \Psi_i^\dagger(x) e^{i\pi\nu \text{sgn}(x-y)}$ and $\Psi_i^\dagger(x) \Psi_i^\dagger(y) = \Psi_i^\dagger(y) \Psi_i^\dagger(x) e^{-i\pi\nu \text{sgn}(x-y)}$ (the rules between operators of different edges are constructed, using Klein factors [39, 41]). The factor $e^{i2\pi\nu}$ is attributed to effective braiding of the thermal anyon around the voltage-biased anyon in the interference $a_2^* a_1$, depicted as the link of two loops in Fig. 2(b); the factorization is equivalent to untying the link. The solid blue loop corresponding to the subcorrelator $\langle \mathcal{T}_{3 \rightarrow 2}^\dagger(t'_2) \mathcal{T}_{3 \rightarrow 2}(t_2) \rangle$ for the thermal anyons is formed, although $t_2 \neq t'_2$, with the help of the thermal length $\hbar v/(k_B T)$; $\langle \mathcal{T}_{3 \rightarrow 2}^\dagger(t'_2) \mathcal{T}_{3 \rightarrow 2}(t_2) \rangle$ is nonvanishing for $|t_2 - t'_2| \lesssim \hbar/(k_B T)$. Similarly, at finite V , the dashed

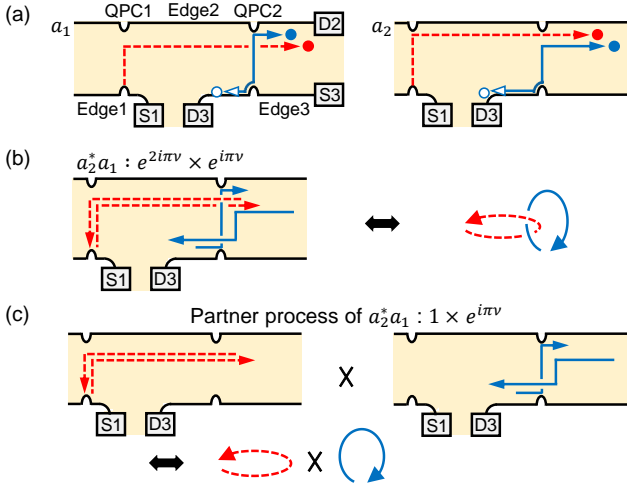


FIG. 2. TVB interference for $W_{3 \rightarrow 2}^{TVB}$. (a) Its subprocesses a_1 and a_2 [identical to those in Fig. 1(c)] have the trajectory (dashed red arrows) of a voltage-biased anyon (red filled circles) and that (solid blue) of a thermal pair excitation of a particle-like anyon (blue filled) and a hole-like anyon (blue empty). Two trajectories are drawn to cross when the corresponding operators are non-commutative due to the fractional statistics. The crossing is time-ordered such that the later trajectory is drawn on top of the earlier one. (b) TVB interference $a_2^* a_1$ between a_1 and a_2 . The trajectories of a_2^* , the complex conjugation of a_2 , are drawn on top of those of a_1 . The loop formed by the dashed red trajectories is topologically linked with that by the solid blue ones, implying effective braiding of the thermal anyon around the voltage-biased anyon. The braiding phase factor is $e^{2i\pi\nu}$. (c) In the partner disconnected process of $a_2^* a_1$, the two loops are unlinked, showing no braiding. $a_2^* a_1$ and its partner have a common phase factor $e^{i\pi\nu}$ due to an exchange of a thermal anyon of a_1 and another of a_2 (the crossing of solid blue trajectories).

red loop representing $\langle \mathcal{T}_{1 \rightarrow 2}^\dagger(t_1) \mathcal{T}_{1 \rightarrow 2}(t_1) \rangle$ for the voltage-biased anyon is formed with $|t_1 - t'_1| \lesssim \hbar\nu/(e^*V)$, when the tunneling at QPC1 occurs at $t'_1 (\neq t_1)$ in a_2 as described by $\mathcal{T}_{1 \rightarrow 2}(t'_1)$. In this case, the braiding occurs for $t'_2 < t_1 + d/v < t_2$ and $t'_2 < t'_1 + d/v < t_2$.

The effective braiding ($e^{2i\pi\nu}$) is decomposed into two events of anyon exchange. One exchange ($e^{i\pi\nu}$) occurs in the subprocess a_1 when the thermal anyon is excited on Edge2 at QPC2 [Fig. 2(a)]. It happens such that the thermal anyon effectively moves from the right side of the voltage-biased anyon to the left on Edge2 [41]. The other ($e^{i\pi\nu}$) occurs in the interference $a_2^* a_1$. The voltage-biased anyon of a_2 moves back to QPC1 passing the thermal anyon of a_1 [the top dashed arrow in Fig. 2(b)].

We call the first term of Eq. (5) a TVB since the trajectory (dashed red loop) of the voltage-biased anyon and that (solid blue loop) of the thermal anyon are disconnected to each other in the conventional sense but topologically linked [35] by the braiding. The TVB is accompanied by a partner *disconnected* process [Fig. 2(c)] that gives the second term of Eq. (5) and has the same

subprocesses as the TVB except the braiding. The TVB and its partner disconnected process (or the correlator in Eq. (5)) appear in our calculation [41] of $W_{i \rightarrow j}$. The pairwise appearance is understood by considering electrons at $\nu = 1$. For the electrons, the TVB is described by a disconnected Feynman diagram as the braiding link has no meaning, $e^{2i\pi\nu} = 1$. Then it must be accompanied and exactly cancelled (leading to $C_{3 \rightarrow 2}^{TVB} = 0$; cf. Eqs. (5) and (6)) by the partner disconnected diagram, following the linked cluster theorem [34]; the second term of Eq. (5) has the minus sign for the cancellation; mathematically, the partner diagram appears due in part to the partition function of a Green's function in its perturbation expansion, hence it does not have the braiding link. For the anyons, the cancellation is partial, because of the braiding.

The common factor of the two terms of Eq. (5) is further factorized with a correlator $D_i(x, t, t') = \langle \Psi_i^\dagger(x, t) \Psi_i(x, t') \rangle$ of each Edge i ,

$$\begin{aligned} & \langle \mathcal{T}_{3 \rightarrow 2}^\dagger(t'_2) \mathcal{T}_{3 \rightarrow 2}(t_2) \rangle \langle \mathcal{T}_{1 \rightarrow 2}^\dagger(t_1) \mathcal{T}_{1 \rightarrow 2}(t_1) \rangle \\ &= e^{i\pi\nu} D_2(d, t_2, t'_2) D_3(0, t_2, t'_2) D_1(0, t_1, t_1) D_2(0, t_1, t_1). \end{aligned} \quad (7)$$

The factor $e^{i\pi\nu}$ comes from exchange of a thermal anyon of a_1 and another of a_2 [Figs. 2(b,c)].

The TVB and its partner disconnected process give

$$W_{3 \rightarrow 2}^{TVB} \propto \gamma_1^2 \gamma_2^2 V^{2\nu-1} T^{2\nu-2} \text{Re}[e^{i\pi\nu} (e^{2i\pi\nu} - 1)], \quad (8)$$

as the thermal (voltage-biased) tunneling probability at QPC2 (QPC1) is proportional to $\gamma_2^2 T^{2\nu-2}$ ($\gamma_1^2 V^{2\nu-2}$) while the current from S1 to QPC1 is proportional to V . The phase factors come from $\text{Re}[C_{3 \rightarrow 2}^{TVB}] \propto \text{Re}[e^{i\pi\nu} (e^{2i\pi\nu} - 1)]$ in Eqs. (5)-(7). $\text{Re}[\dots]$ is taken, considering $[C_{3 \rightarrow 2}^{TVB}]^*$.

There is a TVB process for $W_{2 \rightarrow 3}^{TVB}$. $W_{2 \rightarrow 3}^{TVB}$ is negligibly small at $e^*V \gg k_B T$ [46].

We now compute $\delta S/I$. At $e^*V \gg k_B T$ and $\nu = 1/(2n+1) < 1$, the TVB for $W_{3 \rightarrow 2}^{TVB}$ and its partner disconnected process dominate over the Poisson process for $W_{2 \rightarrow 3}^P$, $W_{3 \rightarrow 2}^{TVB} \gg W_{2 \rightarrow 3}^P$; cf. Eq. (8) and $W_{2 \rightarrow 3}^P \propto \gamma_1^2 \gamma_2^2 V^{4\nu-3}$. Hence, they determine the current and the excess noise, $I = -e^* W_{3 \rightarrow 2}^{TVB}$ and $\delta S = 2(e^*)^2 W_{3 \rightarrow 2}^{TVB}$, leading to Eqs. (1) and (2). We emphasize that the ratio $\delta S/I$ has the negative universal value of $-2e^*$. This originates from the TVB for $W_{3 \rightarrow 2}^{TVB}$ and its partner disconnected process, and equivalently from the anyon braiding. It is nontrivial that the disconnected process contributes to the observables I and δS ; for electrons or bosons, disconnected Feynman diagrams never contribute to observables [34].

The above findings are confirmed by numerically computing δS [41]. For $\nu = 1/3$, δS approaches to $-2e^* I$ such that $\delta S = -1.8e^* I$ at $V = 60 \mu\text{V}$ at 50 mK and $-1.99e^* I$ at $80 \mu\text{V}$ at 50 mK.

Discussion.— The negative excess noise $\delta S < 0$ results from the TVB process for $W_{3 \rightarrow 2}^{TVB}$. It is interpreted as follows. At $V = 0$, tunneling of a particle-like or hole-like

anyon between Edge2 and Edge3 is thermally induced at QPC2, causing the thermal noise $S(0, T)$. Among those tunneling events, thermal tunneling of a hole-like anyon from Edge2 to Edge3 is weakened by a voltage-biased particle-like anyon injected from Edge1 to Edge2, when the voltage V is applied to Edge1. The weakening is due to the effective braiding of the thermal anyon around the voltage-biased anyon, which results in the partial cancellation between the TVB and its partner disconnected process, $W_{3 \rightarrow 2}^{\text{TVB}} \propto \text{Re}[e^{i\pi\nu}(e^{2i\pi\nu} - 1)] < 0$. The weakening leads to the current $I > 0$ and the reduction of the noise $S(V, T)$ below $S(0, T)$. Note that $\delta S < 0$ at any V , although both the Poisson process and the TVB (and its partner) contribute to δS at $e^*V \lesssim k_B T$.

By contrast, for electrons at $\nu = 1$, the Poisson process determines $I = eW_{2 \rightarrow 3}^{\text{P}}$ and $\delta S = 2e^2W_{2 \rightarrow 3}^{\text{P}}$, leading to $\delta S = 2eI > 0$ at $e^*V \gg k_B T$. There is no topological link by the braiding ($e^{2i\pi\nu} = 1$), and the TVB becomes a disconnected process and fully cancelled by its partner disconnected diagram, $W_{i \rightarrow j}^{\text{TVB}} = 0$. This is why the excess noise $\delta S = 2eI$ of the electrons cannot be extrapolated from Eq. (1) with $e^* \rightarrow e$.

Measurement of δS is feasible, as the setup was experimentally studied in other contexts [30–32]: Typically, the tunneling probability of QPC1 and QPC2 is set to be 0.2, to have anyon tunneling [24]. We estimate $I \sim 50$ pA and $\delta S \sim 2.7 \times 10^{-30}$ A²/Hz at 100 μ V and $\nu = 1/3$, which is detectable [30, 47]. When δS is measured by using Eq. (3), one has to experimentally determine temperature T . The determination accuracy is within ± 3 mK [47]. Then, it is possible to obtain $\delta S = -2e^*I(1 \pm 0.2)$ at 50 mK, $V = 80$ μ V, and $\nu = 1/3$.

Our study is generalized to edges with multiple channels or reconstruction (see Ref. [41]). For example, at filling factor $4/3$ or $7/3$ [18, 48], the inner fractional edge channel corresponding to $\nu = 1/3$ interacts with co-propagating outer channels, and is weakly backscattered at the QPCs. In this case δS is still negative. On the other hand, when the $\nu = 1/3$ edge channel interacts with an unexpected counter-propagating mode [49] due to edge reconstruction, δS is negative only when the interaction is sufficiently weak [25, 50]. The outer channels at filling factor $4/3$ or $7/3$ are helpful in this case, since they can screen the edge reconstruction. In the above cases of multiple channels or edge reconstruction, detection of $\delta S < 0$ may imply the fractional statistics of the quasiparticles deviating from Laughlin anyons due to the interchannel interactions. The quasiparticles become closer to Laughlin anyons for weaker interactions.

In summary, we predict the negative excess autocorrelation noise $\delta S < 0$, a signature of the Abelian fractional statistics or the new process (TVB) not existing with fermions or bosons. It is unusual that the excess autocorrelation noise of electrical tunneling current is negative [21, 51].

We suggest that autocorrelation noise can provide sig-

natures [52, 53] of identical-particle statistics. This is different from the conventional approach [54–56] of detecting particle bunching or antibunching with Hanbury Brown-Twiss cross-correlations. It is unnatural to interpret the negative excess autocorrelation noise as deviation (anyonic partial bunching [5–9]) from fermionic antibunching and bosonic bunching, because it originates from the TVB having no counterpart in fermions or bosons.

We thank Hyungkook Choi, Sang-Jun Choi, Yunchul Chung, Sourin Das, Dmitri Feldman, Bertrand Halperin, Charles Kane, and Bernd Rosenow for valuable discussions, and the support by Korea NRF (SRC Center for Quantum Coherence in Condensed Matter, Grant No. 2016R1A5A1008184).

* hssim@kaist.ac.kr

- [1] J. M. Leinaas and J. Myrheim, On the theory of identical particles, *Il Nuovo Cimento B Series* **37**, 1 (1977).
- [2] Daniel Arovas, J. R. Schrieffer, and Frank Wilczek, Fractional Statistics and the Quantum Hall Effect, *Phys. Rev. Lett.* **53**, 722 (1984).
- [3] Ady Stern, Anyons and the quantum Hall effect - a pedagogical review, *Ann. Phys.* **323**, 204 (2008).
- [4] C. de C. Chamon, D. E. Freed, S. A. Kivelson, S. L. Sondhi, and X. G. Wen, Two point-contact interferometer for quantum Hall systems, *Phys. Rev. B* **55**, 2331 (1997).
- [5] I. Safi, P. Devillard, and T. Martin, Partition noise and statistics in the fractional quantum Hall effect, *Phys. Rev. Lett.* **86**, 4628 (2001).
- [6] Smitha Vishveshwara, Revisiting the Hanbury Brown-Twiss Setup for Fractional Statistics, *Phys. Rev. Lett.* **91**, 196803 (2003).
- [7] Eun-Ah Kim, Michael J. Lawler, Smitha Vishveshwara, and Eduardo Fradkin, Signatures of Fractional Statistics in Noise Experiments in Quantum Hall Fluids, *Phys. Rev. Lett.* **95**, 176402 (2005).
- [8] Gabriele Campagnano, Oded Zilberberg, Igor V. Gornyi, Dmitri E. Feldman, Andrew C. Potter, and Yuval Gefen, Hanbury Brown-Twiss Interference of Anyons, *Phys. Rev. Lett.* **109**, 106802 (2012).
- [9] B. Rosenow, I. P. Levkivskyi, and B. I. Halperin, Current Correlations from a Mesoscopic Anyon Collider, *Phys. Rev. Lett.* **116**, 156802 (2016).
- [10] C. L. Kane, Telegraph Noise and Fractional Statistics in the Quantum Hall Effect, *Phys. Rev. Lett.* **90**, 226802 (2003).
- [11] K. T. Law and D. E. Feldman, Electronic Mach-Zehnder interferometer as a tool to probe fractional statistics, *Phys. Rev. B* **74**, 045319 (2006).
- [12] E. Grosfeld, S. H. Simon, and A. Stern, Switching Noise as a Probe of Statistics in the Fractional Quantum Hall Effect, *Phys. Rev. Lett.* **96**, 226803 (2006).
- [13] F. E. Camino, W. Zhou, and V. J. Goldman, $e/3$ Laughlin Quasiparticle Primary-Filling $=1/3$ Interferometer, *Phys. Rev. Lett.* **98**, 076805 (2007).
- [14] D. E. Feldman, Yuval Gefen, Alexei Kitaev, K. T. Law

- and Ady Stern, Shot noise in an anyonic Mach-Zehnder interferometer, *Phys. Rev. B* **76**, 085333 (2007).
- [15] R. L. Willett, L. N. Pfeiffer, and K. W. West, Measurement of filling factor $5/2$ quasiparticle interference with observation of charge $e/4$ and $e/2$ period oscillations, *Proc. Natl. Acad. Sci. U.S.A* **106**, 8853 (2009).
- [16] N. Ofek, A. Bid, M. Heiblum, A. Stern, V. Umansky, and D. Mahalu, Role of interactions in an electronic Fabry Perot interferometer operating in the quantum Hall effect regime, *Proc. Natl. Acad. Sci. U.S.A* **107**, 5276 (2010).
- [17] B. Halperin, A. Stern, I. Neder, and B. Rosenow, Theory of the Fabry-Perot quantum Hall interferometer, *Phys. Rev. B* **83**, 155440 (2011).
- [18] Sanghun An, P. Jiang, H. Choi, W. Kang, S. H. Simon, L. N. Pfeiffer, K. W. West, and K. W. Baldwin, Braiding of Abelian and Non-Abelian Anyons in the Fractional Quantum Hall Effect, [arXiv.org/abs/1112.3400](https://arxiv.org/abs/1112.3400) (2011).
- [19] Bernd Rosenow and Steven H. Simon, Telegraph noise and the Fabry-Perot quantum Hall interferometer, *Phys. Rev. B* **85**, 201302 (2012).
- [20] D. T. McClure, W. Chang, C. M. Marcus, L. N. Pfeiffer, and K. W. West, Fabry-Perot Interferometry with Fractional Charges, *Phys. Rev. Lett.* **108**, 256804 (2012).
- [21] Ya. M. Blanter and M. Büttiker, Shot noise in mesoscopic conductors, *Phys. Rep.* **336**, 1 (2012).
- [22] M. Reznikov, M. Heiblum, Hadas Shtrikman and D. Mahalu, Temporal Correlation of Electrons: Suppression of Shot Noise in a Ballistic Quantum Point Contact, *Phys. Rev. Lett.* **75**, 3340 (1995).
- [23] C. L. Kane and Matthew P. A. Fisher, Nonequilibrium Noise and Fractional Charge in the Quantum Hall Effect, *Phys. Rev. Lett.* **72**, 724 (1994).
- [24] R. de-Picciotto, M. Reznikov, M. Heiblum, V. Umansky, G. Bunin, and D. Mahalu, Direct observation of a fractional charge, *Nature* **389**, 162 (1997).
- [25] L. Saminadayar, D. C. Glatelli, Y. Jin and B. Etienne, Observation of the $e/3$ Fractionally Charged Laughlin Quasiparticle, *Phys. Rev. Lett.* **79**, 2526 (1997).
- [26] M. Reznikov, R. de Picciotto, T. G. Griffiths, M. Heiblum, and V. Umansky, Observation of quasiparticles with one-fifth of an electron's charge, *Nature* **399**, 238 (1999).
- [27] T. G. Griffiths, E. Comferti, M. Heiblum, Ady Stern, and V. Umansky, Evolution of Quasiparticle Charge in the Fractional Quantum Hall Regime, *Phys. Rev. Lett.* **85**, 3918 (2000).
- [28] M. Dolev, M. Heiblum, V. Umansky, Ady Stern and D. Mahalu, Observation of a quarter of an electron charge at the $\nu = 5/2$ quantum Hall state, *Nature* **452**, 829 (2008).
- [29] V. J. Goldman and B. Su, Resonant Tunneling in the Quantum Hall Regime: Measurement of Fractional Charge, *Science* **267**, 1010 (1995).
- [30] E. Comferti, Y. C. Chung, M. Heiblum, V. Umansky, and D. Mahalu, Bunching of Fractionally-Charged Quasiparticles Tunneling through High Potential Barriers, *Nature* **416**, 515 (2002).
- [31] E. Comferti, Y. C. Chung, M. Heiblum, and V. Umansky, Multiple Scattering of Fractionally-Charged Quasiparticles, *Phys. Rev. Lett.* **89**, 066803 (2002).
- [32] Y. C. Chung, M. Heiblum, Y. Oreg, V. Umansky, and D. Mahalu, Anomalous chiral Luttinger liquid behavior of diluted fractionally charged quasiparticles, *Phys. Rev. B* **67**, 201104 (2003).
- [33] There is a theoretical work on the effect of dilute anyon injection on tunneling charges at a QPC in a FQH setup where the QPC is tuned from weak to strong backscattering regimes. See C. L. Kane and Matthew P. A. Fisher, Shot noise and the transmission of dilute Laughlin quasiparticles, *Phys. Rev. B* **67**, 045307 (2003). This work does not discuss any effect of the anyon fractional statistics. By contrast, in our study we propose to use dilute anyon injection for observing the fractional statistics, focusing on the weak backscattering regime of QPCs.
- [34] For bosons and fermions, disconnected diagrams never contribute to observables. See, e.g., A. L. Fetter and J. D. Walecka, *Quantum theory of many-particle systems*. (McGraw-Hill, New York, 1971).
- [35] Disconnected diagrams but linked by braiding appear in the algebraic theory of anyons. See, e.g., J. Preskill, *Lecture Notes for Physics 219: Quantum Computation* (California Institute of Technology, Pasadena CA 1998) URL: <http://www.theory.caltech.edu/people/preskill/ph219/>. See also A. Kitaev, Anyons in an exactly solved model and beyond, *Ann. Phys.* **321**, 2 (2006).
- [36] C. Han, J. Park, Y. Gefen, and H.-S. Sim, Topological vacuum bubbles by anyon braiding, *Nat. Commun.* **7**, 11131 (2016). While this previous work studied the transport mechanism of a Fabry-Perot interference current in a three-QPC setup, the present work predicts a new mechanism of shot noise at a single QPC in the simpler two-QPC setup.
- [37] X. G. Wen, Chiral Luttinger liquid and the edge excitations in the fractional quantum Hall states, *Phys. Rev. B* **41**, 12838 (1990).
- [38] J. von Delft and H. Schoeller, Bosonization for Beginners—Refermionization for Experts, *Ann. Phys. (Leipzig)* **7**, 225 (1998).
- [39] R. Guyon, P. Devillard, T. Martin, and I. Safi, Klein factors in multiple fractional quantum Hall edge tunneling, *Phys. Rev. B* **65**, 153304 (2002).
- [40] Note that the correction of order $O(T/V)$ to Eq. (1) is found as $\delta S/I = -2e^* [1 + \frac{4\nu(1-2\nu)}{\sin 2\pi\nu} \frac{\pi k_B T}{e^* V}]$. It occurs due to the spatial broadening $\hbar v/(e^* V)$ of the voltage-biased anyon that leads to imperfection of the effective braiding.
- [41] See Supplemental Material for the Hamiltonian and operators of the setup, the Klein factors, the expression of $f(\nu)$, the derivation of Eqs. (3) and (6), the effective braiding, the detailed computation of $W_{i \rightarrow j}$, the correction of order $O(T/V)$ to Eq. (1), and the effect of multiple edge channels and edge reconstruction.
- [42] Chenjie Wang and D. E. Feldman, Fluctuation-dissipation theorem for chiral systems in nonequilibrium steady states, *Phys. Rev. B* **84**, 235315 (2011).
- [43] Chenjie Wang and D. E. Feldman, Chirality, Causality, and Fluctuation-Dissipation Theorems in Nonequilibrium Steady States, *Phys. Rev. Lett.* **110**, 030602 (2013).
- [44] O. Smits, J. K. Slingerland, and S. H. Simon, Nonequilibrium noise in the (non-)Abelian fractional quantum Hall effect, arxiv.org/pdf/1401.4581.
- [45] D. E. Feldman and M. Heiblum, Why a noninteracting model works for shot noise in fractional charge experiments, *Phys. Rev. B* **95**, 115308 (2017).
- [46] The TVB process for $W_{2 \rightarrow 3}^{\text{TVB}}$ is identical to that of $W_{3 \rightarrow 2}^{\text{TVB}}$, except that its thermal anyons move in the opposite direction to those of $W_{3 \rightarrow 2}^{\text{TVB}}$. $W_{2 \rightarrow 3}^{\text{TVB}}$ has the same expression as $W_{3 \rightarrow 2}^{\text{TVB}}$ in Eq. (8), but with the replacement of $e^{2i\pi\nu} \rightarrow e^{-2i\pi\nu}$.

- [47] Private communication with Y. C. Chung and H.-K. Choi. Current $\gtrsim 0.5$ pA and noise $\gtrsim 10^{-30}$ A²/Hz are well detectable.
- [48] S. Baer, C. Rössler, T. Ihn, K. Ensslin, C. Reichl, and W. Wegscheider, Experimental prove of topological orders and edge excitations in the second Landau Level, *Phys. Rev. B* **90**, 075403 (2014).
- [49] B. Rosenow and B. I. Halperin, Nonuniversal Behavior of Scattering between Fractional Quantum Hall Edges, *Phys. Rev. Lett.* **88**, 096404 (2002).
- [50] Stefano Roddaro, Vittorio Pellegrini, and Fabio Beltram, Nonlinear Quasiparticle Tunneling between Fractional Quantum Hall Edges, *Phys. Rev. Lett.* **90**, 046805 (2003).
- [51] For noninteracting electrons, a negative excess noise can appear, not originating from the fermionic statistics, in a certain situation irrelevant to our case. See, e.g., G. B. Lesovik and R. Loosen, Negative excess noise in quantum conductors, *Z. Phys. B* **91**, 531 (1993). See also F. Dolcini and H. Grabert, Tuning Excess Noise by Aharonov-Bohm Interferometry, *Chem. Phys.* **375**, 291 (2010).
- [52] Negative excess noise can occur due to the bosonic statistics. See, e.g., M. Büttiker, Scattering theory of current and intensity noise correlations in conductors and wave guides, *Phys. Rev. B* **46**, 12485 (1992). See also John H. Davies, Per Hylgaard, Selman Hershfild, and John W. Wilkins, Classical theory for shot noise in resonant tunneling, *Phys. Rev. B* **46**, 9620 (1992).
- [53] Generalization of our results to non-Abelian statistics is in progress. Byeongmok Lee, Cheolhee Han, and H.-S. Sim, in preparation.
- [54] M. Henny, S. Oberholzer, C. Strunk, T. Heinzel, K. Ensslin, M. Holland, and C. Schönenberger, The Fermionic Hanbury Brown and Twiss Experiment, *Science* **284**, 296 (1999).
- [55] W. D. Oliver, J. Kim, R. C. Liu, Y. Yamamoto, Hanbury Brown and Twiss-Type Experiment with Electrons, *Science* **284**, 299 (1999).
- [56] T. Jelts, J. M. McNamara, W. Hogervorst, W. Vassen, V. Krachmalnicoff, M. Schellekens, A. Perrin, H. Chang, D. Boiron, A. Aspect, and C. I. Westbrook, Comparison of the Hanbury Brown-Twiss effect for bosons and fermions, *Nature* **445**, 402 (2007).

Supplemental Material : Negative excess shot noise by anyon braiding

Byeongmok Lee,¹ Cheolhee Han,¹ and H.-S. Sim^{1,*}

¹*Department of Physics, Korea Advanced Institute of Science and Technology, Daejeon 34141, Korea*

(Dated: December 4, 2021)

This material includes the Hamiltonian and operators of the setup, the Klein factors, the expression of $f(\nu)$, the derivation of Eqs. (3) and (6), the effective braiding, the detailed expression and computation of $W_{i \rightarrow j}$, the correction of order $O(T/V)$ to Eq. (1), and the effect of multiple edge channels and edge reconstruction.

Hamiltonian and operators of the setup, and Klein factors

The Hamiltonian of the setup is

$$H = \sum_i H_i + H_{\text{tun}}. \quad (\text{S1})$$

Edge i is described by the chiral Luttinger liquid [1, 2] $H_i = \frac{\hbar v}{4\pi\nu} \int_{-\infty}^{\infty} dx : (\partial_x \phi_i(x))^2 : + e^* V_i \hat{N}_i$, the anyon operator $\Psi_i^\dagger(x, t) = F_i^\dagger(t) e^{-i\phi_i(x, t)} / \sqrt{2\pi a}$ by the boson field $\phi_i(x)$, and anyon tunneling at the QPCs by $H_{\text{tun}} = \gamma_1(\mathcal{T}_{1 \rightarrow 2} + \mathcal{T}_{1 \rightarrow 2}^\dagger) + \gamma_2(\mathcal{T}_{2 \rightarrow 3} + \mathcal{T}_{2 \rightarrow 3}^\dagger)$. Here, $V_1 = V$, $V_{2,3} = 0$, \hat{N}_i is the anyon number operator obeying $[N_i, F_j^\dagger] = \delta_{ij} F_i^\dagger$, a is the short-length cutoff, and F_i^\dagger is the Klein factor [16] satisfying $F_i^\dagger F_i = 1$, $F_1(t) = F_1(0) e^{-ie^* V t / \hbar}$, and $[\phi_i, F_j] = 0$. The exchange rule between anyons on different edges is achieved with the commutators of F_i ,

$$\begin{aligned} F_1 F_2 &= F_2 F_1 e^{i\pi\nu}, & F_2 F_3 &= F_3 F_2 e^{i\pi\nu}, & F_1 F_3 &= F_3 F_1 e^{i\pi\nu}, \\ F_1^\dagger F_2 &= F_2 F_1^\dagger e^{-i\pi\nu}, & F_2^\dagger F_3 &= F_3 F_2^\dagger e^{-i\pi\nu}, & F_1^\dagger F_3 &= F_3 F_1^\dagger e^{-i\pi\nu}. \end{aligned} \quad (\text{S2})$$

We treat H_{tun} as a perturbation on $\sum_i H_i$. The operators for I and S at QPC2 are $\hat{I} = ie^* \gamma_2 (\mathcal{T}_{2 \rightarrow 3} - \mathcal{T}_{2 \rightarrow 3}^\dagger) / \hbar$, $\hat{S} = \int_{-\infty}^{\infty} dt \delta \hat{I}(0) \delta \hat{I}(t) + \delta \hat{I}(t) \delta \hat{I}(0)$, and $\delta \hat{I}(t) = \hat{I}(t) - I$.

We attach the Klein factors in Eq. (S2), utilizing the connected-edge scheme [16]. The connected edge is constructed by gluing Edge1, Edge2, and Edge3, and it has the same chirality with Edge i 's. Here, Edge i 's are regarded as part of the boundary (which is the connected edge) of one fractional quantum Hall liquid. Then the commutation rule between the boson field $\phi_2(x_2)$ of Edge2 and the boson field $\phi_3(x_3)$ of Edge3, for example, can be assigned, following the commutation rule $[\phi(z_2), \phi(z_3)] = i\pi\nu \text{sgn}(z_2 - z_3)$ of the corresponding boson field ϕ of the connected edge of coordinate z (see Fig. S1). Similarly, the commutation rule between the quasiparticle operators of two different edges can be assigned. This leads to Eq. (S2).

We note that for our setup, one can omit the Klein factors in the limiting case where the distance between QPC1 and QPC2 in Edge2 is infinite (much longer than the spatial broadening of thermal anyons and voltage-biased anyons). In this case, it is enough to compute the correlator of the form $\langle \mathcal{T}_{1 \rightarrow 2}^\dagger(t_1) \mathcal{T}_{3 \rightarrow 2}^\dagger(t'_2) \mathcal{T}_{3 \rightarrow 2}(t_2) \mathcal{T}_{1 \rightarrow 2}(t_1) \rangle$ (see Eq. (5) in the main text) for the calculation of I and δS . In the computation of the correlator, the Klein factor occurring in $\mathcal{T}_{3 \rightarrow 2}(t_2) \mathcal{T}_{1 \rightarrow 2}(t_1)$ is the same with, hence cancels exactly, that in $\mathcal{T}_{3 \rightarrow 2}(t'_2) \mathcal{T}_{1 \rightarrow 2}(t_1)$. Hence the same computation result is obtained without introducing the Klein factors.

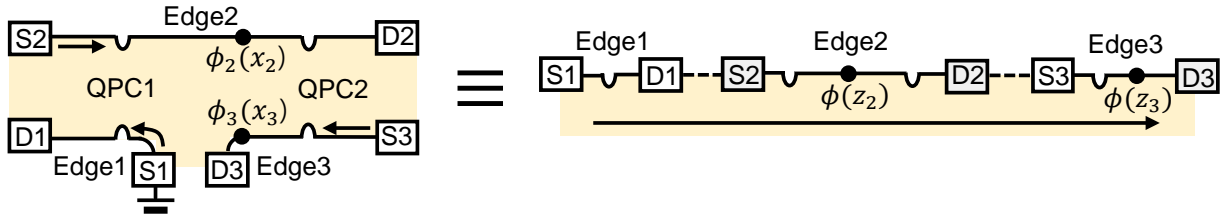


FIG. S1: A single connected edge (the right panel) equivalent with our setup (the left). The dashed line between D1 and S2 in the right panel represents the edge connecting Edge1 and Edge2, and the dashed line between D2 and S3 shows the edge connecting Edge2 and Edge3. The connected edge has the same chirality (see the arrows) with Edge1, Edge2, and Edge3.

On the other hand, however, when the distance between QPC1 and QPC2 is short, the correlators of the other forms, such as $\langle \mathcal{T}_{3 \rightarrow 2}^\dagger(t'_2) \mathcal{T}_{1 \rightarrow 2}^\dagger(t_1) \mathcal{T}_{3 \rightarrow 2}(t_2) \mathcal{T}_{1 \rightarrow 2}(t_1) \rangle$, contribute to I and δS , and the calculation of the correlators requires the Klein factors. The fractional exchange phase $e^{i\pi\nu}$ of the Klein factors in Eq. (S2) and that of anyons on the same edges together result in the negative excess noise. To distinguish the contribution of the fractional exchange phase of the Klein factors to I and δS from that of anyon exchange on the same edge, we substitute ν 's in Eq. (S2) with ν_K and recalculate I and δS for the limiting case where the distance between QPC1 and QPC2 goes to zero,

$$\begin{aligned} I &\simeq e^* \gamma_1^2 \gamma_2^2 f(\nu) [\cos(\pi\nu - \pi(\nu + \nu_K)) - \cos(\pi\nu + \pi(\nu + \nu_K))] V^{2\nu-1} T^{2\nu-2}, \\ \delta S &\simeq -e^{*2} \gamma_1^2 \gamma_2^2 f(\nu) [2\cos(\pi\nu) - \cos(\pi\nu - \pi(\nu + \nu_K)) - \cos(\pi\nu + \pi(\nu + \nu_K))] V^{2\nu-1} T^{2\nu-2}. \end{aligned} \quad (\text{S3})$$

The above equation is identical to Eq. (2) of the main text if one replaces ν_K by ν . One has a wrong result if one omits the exchange phase of the Klein factors in the case that the distance between the two QPCs is finite. The equation (S3) shows that the exchange phase $\pi\nu_K$ of the Klein factors constitutes one half of the braiding phase of the topological vacuum bubbles (TVBs), while the exchange phase of anyons on the same edge results in the other half. Therefore, one needs to introduce the Klein factors in the general situations of our setup.

$f(\nu)$ in Eq. (2)

In Eq. (2) in the main text, $f(\nu) = \pi^{2\nu-9/2} e^{*2\nu-1} v^{-4\nu} \hbar^{-4\nu-1} (k_B a^2)^{2\nu-2} \cot(\pi\nu) \Gamma(\nu) \Gamma(1/2 - \nu) / [16\Gamma(2\nu)]$. $\Gamma(\nu)$ is the Gamma function.

Derivation of Eq. (3)

We derive Eq. (3) in the main text. The current at D3 satisfies $I_3 = I_{\text{in}} + I$ due to current conservation. $I_{\text{in}} = \overline{I_{\text{in}}(t)}$ is the average current from S3 to QPC2 along Edge3. The noise at D3 is decomposed as $S_3 = S + 2S_{3,\text{in}} + S_{\text{in}}$, where $S_{\text{in}} = 2 \int_{-\infty}^{\infty} dt \delta I_{\text{in}}(t) \delta I_{\text{in}}(0)$, $S_{3,\text{in}} = 2 \int_{-\infty}^{\infty} dt \delta I_{\text{in}}(t) \delta I(0)$, and $\delta I_{\text{in}}(t) = I_{\text{in}}(t) - I_{\text{in}}$. S_{in} is the half of the Johnson-Nyquist noise $4k_B T \nu e^2 / h$ and independent of V , hence, it does not appear in Eq. (3) in the main text. $2S_{3,\text{in}}$ is the correlation between the tunneling current I at QPC2 and the current I_{in} from S3 to QPC2 and written as the second or fourth term of Eq. (3) in the main text, according to the nonequilibrium fluctuation-dissipation theorem [4–6].

Derivation of Eq. (6)

In the derivation of Eq. (6) in the main text, we used the identity [1] $\langle e^{s_1 \phi_1} e^{s_2 \phi_2} \dots \rangle = e^{\sum_j s_j^2 \langle \phi_j^2 \rangle + \sum_{i < j} s_i s_j \langle \phi_i \phi_j \rangle}$ with $s_i = \pm i$.

Expression and computation of $W_{i \rightarrow j}$

Using the Keldysh method [7, 8], $W_{i \rightarrow j}$ is expressed as

$$\begin{aligned} W_{3 \rightarrow 2} &= -\gamma_1^2 \gamma_2^2 \sum_{\eta_3 \eta_4 = \pm 1} \eta_3 \eta_4 \text{Re} \left[\int_{-\infty}^{\infty} dt'_2 dt_1 dt'_1 \right. \\ &\quad \left. \langle T_K \mathcal{T}_{3 \rightarrow 2}(t_2^{\eta_1=1}) \mathcal{T}_{3 \rightarrow 2}^\dagger(t_2'^{\eta_2=-1}) \mathcal{T}_{1 \rightarrow 2}(t_1^{\eta_3}) \mathcal{T}_{1 \rightarrow 2}^\dagger(t_1'^{\eta_4}) \rangle \right] \\ W_{2 \rightarrow 3} &= -\gamma_1^2 \gamma_2^2 \sum_{\eta_3 \eta_4 = \pm 1} \eta_3 \eta_4 \text{Re} \left[\int_{-\infty}^{\infty} dt'_2 dt_1 dt'_1 \right. \\ &\quad \left. \langle T_K \mathcal{T}_{3 \rightarrow 2}^\dagger(t_2^{\eta_1=1}) \mathcal{T}_{3 \rightarrow 2}(t_2'^{\eta_2=-1}) \mathcal{T}_{1 \rightarrow 2}^\dagger(t_1^{\eta_3}) \mathcal{T}_{1 \rightarrow 2}(t_1'^{\eta_4}) \rangle \right] \end{aligned} \quad (\text{S4})$$

upto the leading order $O(\gamma_1^2 \gamma_2^2)$ of the perturbation, where η_i 's are Keldysh indices, T_K means the Keldysh ordering, and $t_2 = 0$ is chosen.

We compute $W_{i \rightarrow j}$ analytically to get Eq. (2) of the main text and also numerically. The analytic calculation can be done [9, 10] at $e^* V \gg k_B T$ where $W_{i \rightarrow j}$ is determined by the narrow domain of $|t_1 - t'_1| \lesssim \hbar / (e^* V)$, as t_1

(t'_1) is the time of injection of a particle-like anyon from Edge1 to Edge2 in subprocess a_1 (a_2). The Poisson process for $W_{2 \rightarrow 3}^P$ occurs in the domain $t_2 \simeq t'_2 \simeq t_1 + d/v \simeq t'_1 + d/v$ of the terms $\eta_3 = -\eta_4 = -1$ of $W_{2 \rightarrow 3}$ in Eq. (S4). The TVB (its partner disconnected process) for $W_{3 \rightarrow 2}^{\text{TVB}}$ occurs in the domain $t'_2 < t_1 + d/v \simeq t'_1 + d/v < t_2$ and $t_2 < t_1 + d/v \simeq t'_1 + d/v < t'_2$ of the terms $\eta_3 = -\eta_4 = -1$ ($\eta_3 = \eta_4 = \pm 1$) of $W_{3 \rightarrow 2}$. The first (second) term of Eq. (5) in the main text is found from a term with $\eta_3 = -\eta_4 = -1$ ($\eta_3 = \eta_4 = 1$) at $t'_1 \rightarrow t_1$. The TVB and its partner for $W_{2 \rightarrow 3}^{\text{TVB}}$ similarly occur in $W_{2 \rightarrow 3}$.

Leading-order correction to Eqs. (1) and (2)

We obtain the corrections of the leading order $O(T/V)$ to Eqs. (1) and (2) below. At $e^*V \gg k_B T$, the corrections to the tunneling current I and the excess noise δS are found as

$$I \simeq e^* \gamma_1^2 \gamma_2^2 f(\nu) [\cos(\pi\nu) - \cos(3\pi\nu)] V^{2\nu-1} T^{2\nu-2} \left[1 - 2\nu(1-2\nu) \tan(\pi\nu) \frac{\pi k_B T}{e^* V} \right], \quad (\text{S5})$$

$$\delta S \simeq -2e^{*2} \gamma_1^2 \gamma_2^2 f(\nu) [\cos(\pi\nu) - \cos(3\pi\nu)] V^{2\nu-1} T^{2\nu-2} \left[1 + 2\nu(1-2\nu) \cot(\pi\nu) \frac{\pi k_B T}{e^* V} \right]. \quad (\text{S6})$$

Combining the results, we find the leading-order correction to Eq. (1),

$$\frac{\delta S}{I} = -2e^* \left[1 + \frac{4\nu(1-2\nu)}{\sin 2\pi\nu} \frac{\pi k_B T}{e^* V} \right]. \quad (\text{S7})$$

Effective braiding

The effective braiding phase factor $e^{2i\pi\nu}$ in Eq. (6) can be understood by using the connected-edge scheme in Fig. S1. One half $e^{i\pi\nu}$ of the phase factor is gained in the subprocess a_1 . Here, a pair of a voltage-biased particle-like anyon and its hole-like partner is excited at QPC1, and then the anyons propagate. This process, described by the tunneling operator $T_{1 \rightarrow 2}(t_1)$, is drawn on the connected edge in the right panel of Fig. S2(a). After the voltage-biased particle-like anyon passes QPC2, a pair of thermal particle-like and hole-like anyons is excited at QPC2. This is described by $T_{3 \rightarrow 2}(t_2)$. The resulting configuration of the four anyons by $T_{3 \rightarrow 2}(t_2)T_{1 \rightarrow 2}(t_1)$ is shown in Fig. S2(b). Notice that the thermal particle-like anyon is in the left side of the voltage-biased particle-like anyon on the connected edge, while the thermal hole-like anyon is created in the right side. This is equivalent with the following situation: The thermal particle-like and hole-like anyons are created from the vacuum on the right side of the voltage-biased particle-like anyon, and then the thermal particle-like anyon moves to the left side. In this anyon exchange, a phase factor $e^{i\pi\nu}$ is gained. This is the one half of the braiding phase factor, and obtained partly by a Klein factor in the computation.

On the other hand, the other half $e^{i\pi\nu}$ of the braiding phase factor is gained in interference $a_2^* a_1$ between a_1 and a_2 . In a_2 , a pair of a voltage-biased particle-like anyon and its hole-like partner is excited at QPC1, and then the anyons propagate. This is described by $T_{1 \rightarrow 2}(t_1)$. Before the voltage-biased particle-like anyon passes QPC2, a pair of

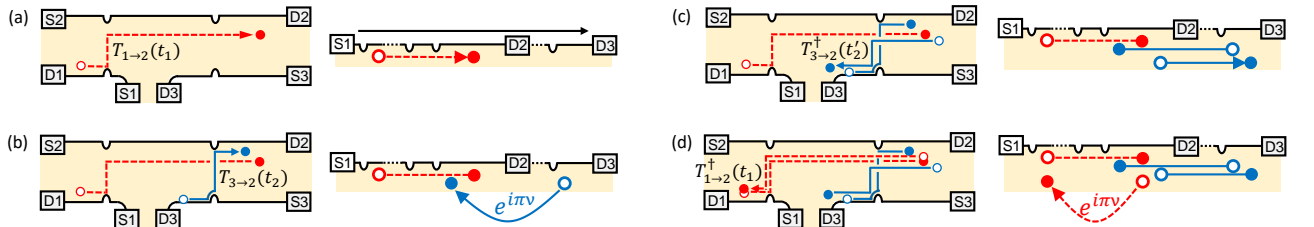


FIG. S2: Anyon propagations in the subprocesses [the left panels of (a-d)] of the interference $a_2^* a_1$ are drawn on the connected edge [the right panels] corresponding to our setup. We used the connected-edge scheme in Fig. S1. A voltage-biased particle-like (hole-like) anyon is depicted by the filled (empty) red circles. A thermal particle-like (hole-like) anyon is drawn as the filled (empty) blue circles.

thermal particle-like and hole-like anyons is excited at QPC2. This is described by $T_{3 \rightarrow 2}(t'_2)$. In the interference $a_2^* a_1$ described by $T_{1 \rightarrow 2}^\dagger(t_1) T_{3 \rightarrow 2}^\dagger(t'_2) T_{3 \rightarrow 2}(t_2) T_{1 \rightarrow 2}(t_1)$, we consider the complex-conjugated process of a_2 , $T_{1 \rightarrow 2}^\dagger(t_1) T_{3 \rightarrow 2}^\dagger(t'_2)$. On top of the anyon configuration of the subprocess a_1 [$T_{3 \rightarrow 2}(t_2) T_{1 \rightarrow 2}(t_1)$; see Fig. S2(b)], we first draw the anyon configuration corresponding the excitation of the thermal anyon pair of a_2^* on the connected edge [see Fig. S2(c)]. Here, the pair is created in the outside of the dashed line between the voltage-biased particle-like anyon and its hole-like partner. Therefore, no anyon exchange happens between the voltage-biased anyons and the thermal anyons in this step. We next draw the voltage-biased anyon pair of a_2^* on the connected edge [see Fig. S2(d)]. We notice that the voltage-biased particle-like anyon is created in the left side of the thermal particle-like anyon of a_1 , while the voltage-biased hole-like anyon occurs in the right side. This is equivalent with the following situation: The voltage-biased particle-like and hole-like anyons of a_2^* are created from the vacuum on the right side of the thermal particle-like anyon of a_1 , and then the voltage-biased particle-like anyon moves to the left side. In this anyon exchange, a phase factor $e^{i\pi\nu}$ is gained. This is the other half of the braiding phase factor.

Effects of an additional co-propagating (downstream) outer edge channel

We consider the situation where there is an additional co-propagating (downstream) outer channel along Edge1, Edge2, and Edge3. This situation can occur in fractional quantum Hall systems of, e.g., filling factor $7/3 = 2 + 1/3$ or $4/3 = 1 + 1/3$ [12, 13]. In this situation, the negative excess noise $\delta S < 0$ is still found. The value of δS depends on the inter-channel interaction strength and the distance between QPC1 and QPC2 in Edge2. The negative excess noise provides a signature of the fractional statistics of anyons in the inner channel. We expect that the outer channel is helpful for observing the negative excess noise, since it can screen the effect [11] of edge reconstruction or upstream neutral modes; the effect of the neutral modes will be discussed in the next section.

The Hamiltonian in Eq. (S1) is modified as $H = \sum_i H_i + H_{i,\text{out}} + H_{\text{tun}}$ to include the additional outer edge channel,

$$H_{i,\text{out}} = \frac{\hbar v_{\text{out}}}{4\pi\nu_{\text{out}}} \int_{-\infty}^{\infty} dx : (\partial_x \phi_{i,\text{out}}(x))^2 : + \frac{\hbar\kappa}{2\pi} \int_{-\infty}^{\infty} dx \partial_x \phi_i(x) \partial_x \phi_{i,\text{out}}(x). \quad (\text{S8})$$

The first term is the Hamiltonian of the outer edge channel, and the second term describes the interaction between the density $\partial_x \phi_i(x)$ of the inner edge channel and the density $\partial_x \phi_{i,\text{out}}(x)$ of the outer channel. v_{out} is the velocity of the outer channel, ν_{out} is the effective filling factor for the outer channel, and κ is the inter-channel interaction strength. The commutation relations of the boson fields are

$$[\phi_i(x), \phi_i(x')] = i\pi\nu \text{sign}(x - x'), \quad [\phi_{i,\text{out}}(x), \phi_{i,\text{out}}(x')] = i\pi\nu_{\text{out}} \text{sign}(x - x'), \quad [\phi_i(x), \phi_{i,\text{out}}(x')] = 0. \quad (\text{S9})$$

As in the case of the single edge channel per edge, anyon tunneling occurs between the inner channels (described by $\phi_i(x)$'s) of Edge1 and Edge2 at QPC1, and between the inner channels of Edge2 and Edge3 at QPC2, and we treat the tunneling Hamiltonian H_{tun} as a perturbation on $\sum_i H_i + H_{i,\text{out}}$.

The bare Hamiltonian $\sum_i H_i + H_{i,\text{out}}$ is diagonalized as

$$H_i + H_{i,\text{out}} = \frac{\hbar v_1}{4\pi\nu_1} \int_{-\infty}^{\infty} dx : (\partial_x \phi_{i1}(x))^2 : + \frac{\hbar v_2}{4\pi\nu_2} \int_{-\infty}^{\infty} dx : (\partial_x \phi_{i2}(x))^2 : + e^* V_i \hat{N}_i \quad (\text{S10})$$

$$\begin{pmatrix} \phi_i(x) \\ \phi_{i,\text{out}}(x) \end{pmatrix} = \begin{pmatrix} T_{11} & T_{12} \\ T_{21} & T_{22} \end{pmatrix} \begin{pmatrix} \phi_{i1}(x) \\ \phi_{i2}(x) \end{pmatrix} \quad (\text{S11})$$

where the commutation relations for the new boson fields are

$$[\phi_{i1}(x), \phi_{i1}(x')] = i\pi\nu_1 \text{sign}(x - x'), \quad [\phi_{i2}(x), \phi_{i2}(x')] = i\pi\nu_2 \text{sign}(x - x'), \quad [\phi_{i1}(x), \phi_{i2}(x')] = 0. \quad (\text{S12})$$

The elements of the transformation matrix T are found as

$$\begin{aligned} T_{11} &= \left[\frac{\nu}{2} \left(1 + \frac{(v - v_{\text{out}})}{\sqrt{(v - v_{\text{out}})^2 + 4\kappa^2 \nu \nu_{\text{out}}}} \right) \right]^{1/2}, & T_{12} &= \left[\frac{\nu}{2} \left(1 - \frac{(v - v_{\text{out}})}{\sqrt{(v - v_{\text{out}})^2 + 4\kappa^2 \nu \nu_{\text{out}}}} \right) \right]^{1/2} \\ T_{21} &= \left[\frac{\nu_{\text{out}}}{2} \left(1 - \frac{(v - v_{\text{out}})}{\sqrt{(v - v_{\text{out}})^2 + 4\kappa^2 \nu \nu_{\text{out}}}} \right) \right]^{1/2}, & T_{22} &= - \left[\frac{\nu_{\text{out}}}{2} \left(1 + \frac{(v - v_{\text{out}})}{\sqrt{(v - v_{\text{out}})^2 + 4\kappa^2 \nu \nu_{\text{out}}}} \right) \right]^{1/2}. \end{aligned} \quad (\text{S13})$$

Using the diagonalized form, we obtain the correlator $\langle \phi_i(0,0)\phi_i(x,t) \rangle_0$ useful for computing the current I and the excess noise δS ,

$$\begin{aligned} \langle \phi_i(0,0)\phi_i(x,t) \rangle_0 &= \langle (T_{11}\phi_{i1}(0,0) + T_{12}\phi_{i2}(0,0)) (T_{11}\phi_{i1}(x,t) + T_{12}\phi_{i2}(x,t)) \rangle_0 \\ &= T_{11}^2 \langle \phi_{i1}(0,0)\phi_{i1}(x,t) \rangle_0 + T_{12}^2 \langle \phi_{i2}(0,0)\phi_{i2}(x,t) \rangle_0 = \ln \left[\left(\frac{\tau_0 + i(t-x/v_1)}{\tau_0} \right)^{T_{11}^2} \left(\frac{\tau_0 + i(t-x/v_2)}{\tau_0} \right)^{T_{12}^2} \right], \end{aligned} \quad (\text{S14})$$

where

$$v_1 = \frac{v + v_{\text{out}} + \sqrt{(v - v_{\text{out}})^2 + 4\kappa^2\nu\nu_{\text{out}}}}{2}, \quad v_2 = \frac{v + v_P - \sqrt{(v - v_{\text{out}})^2 + 4\kappa^2\nu\nu_{\text{out}}}}{2}. \quad (\text{S15})$$

Using the correlator, we obtain $\delta S/I$ at $e^*V \gg k_B T$,

$$\frac{\delta S}{I} = -2e^* \cot(\pi\nu) \frac{[1 - \cos(2\pi\nu)]e^{-Ad} + [2 - \cos(2\pi T_{11}^2) - \cos(2\pi T_{12}^2)](1 - e^{-Ad})}{\sin(2\pi\nu)e^{-Ad} + [\sin(2\pi T_{11}^2) + \sin(2\pi T_{12}^2)](1 - e^{-Ad})}, \quad (\text{S16})$$

where $e^* = \nu e$, $A = 2\nu \left(\frac{1}{v_2} - \frac{1}{v_1} \right) \pi T$, and d is the distance between QPC1 and QPC2 on Edge2. When $d = 0$, we find $\delta S/I = -2e^*$, which is independent of the inter-channel interaction strength κ and the properties (such as v_{out} and ν_{out}) of the outer edge channel. On the other hand, in the case of $d \rightarrow \infty$ (much longer than the spatial broadening of thermal anyons excited at QPC2), $\delta S/I$ increases with increasing the interaction strength κ . At $\kappa \rightarrow \infty$ and $d \rightarrow \infty$, $\delta S/I$ converges to

$$\frac{\delta S}{I} \rightarrow -2e^* \cot(\pi\nu) \frac{1 - \cos(\pi\nu)}{\sin(\pi\nu)}. \quad (\text{S17})$$

For example, at $\nu = 1/3$ (i.e., at the filling factor $4/3 = 1 + 1/3$ or $7/3 = 2 + 1/3$), $\delta S/I = -2e^*/3$ at $\kappa \rightarrow \infty$ and $d \rightarrow \infty$. See Fig. S3(a). This shows that the excess noise is always negative even in the presence of additional co-propagating (downstream) channels along the edges.

Effects of edge reconstruction

In this section, we study the effect of edge reconstruction. The edge reconstruction can result in upstream outer channels [11]. To see the effect, we consider the situation where there is an additional upstream outer channel along each edge (instead of an additional downstream channel as in the last section). In this situation, the excess noise δS is negative only when the interchannel interaction strength is sufficiently weak. We also discuss the possibility of observing the negative excess noise $\delta S < 0$ in the situation of some reported experiments.

The Hamiltonian in Eq. (S1) is now modified as $H = \sum_i H_i + H_{i,P} + H_{\text{tun}}$. The term $H_{i,P}$ describes the upstream outer channel (which is a phonon mode in Ref. [11]) and its interaction with the downstream inner channel,

$$H_{i,P} = \frac{\hbar v_P}{4\pi\nu_P} \int_{-\infty}^{\infty} dx : (\partial_x \phi_{i,P}(x))^2 : + \frac{\hbar\kappa}{2\pi} \int_{-\infty}^{\infty} dx \partial_x \phi_i(x) \partial_x \phi_{i,P}(x). \quad (\text{S18})$$

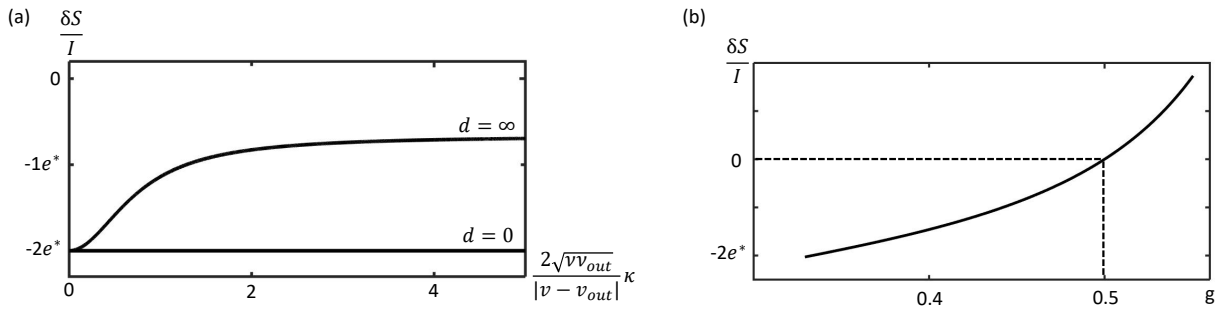


FIG. S3: (a) Current-to-noise ratio $\delta S/I$ as a function of the normalized interaction strength $\frac{2\sqrt{\nu\nu_{\text{out}}}}{|v-v_{\text{out}}|} \kappa$ in the case of an additional downstream (co-propagating) edge channel. $\nu = 1/3$ is chosen, while ν_{out} is arbitrary. (b) $\delta S/I$ as a function of the exponent g of the current-voltage characteristics of anyon tunneling at the QPCs in the presence of edge reconstruction. $\nu = 1/3$ is chosen.

It has the same form as $H_{i,\text{out}}$ in Eq. (S8). The upstream outer channel is described by the boson field $\phi_{i,\text{P}}$. The commutation relations of the boson fields are

$$[\phi_i(x), \phi_i(x')] = i\pi\nu\text{sign}(x - x') \quad [\phi_{i,\text{P}}(x), \phi_{i,\text{P}}(x')] = -i\pi\nu_{\text{P}}\text{sign}(x - x') \quad [\phi_i(x), \phi_{i,\text{P}}(x')] = 0 \quad (\text{S19})$$

The minus sign in the second commutation relation implies the upstream flow of the outer channel.

Following the steps discussed in the last section, we obtain

$$\frac{\delta S}{I} = -2e^* \frac{\tan \frac{\pi(\nu+g)}{2}}{\tan(\pi g)} \quad (\text{S20})$$

for $g < 1$. Here $g = \frac{\nu(v+v_P)}{\sqrt{(v+v_P)^2 - 4\kappa^2\nu\nu_P}}$ is the exponent of the relation [2] $\mathcal{I} \sim \mathcal{V}^{2g-1}$ of anyon tunneling current \mathcal{I} between two edges at a QPC by a bias voltage \mathcal{V} . In the absence of the edge reconstruction, g is identical to the filling factor ν (in the case of the Laughlin-sequence filling factors), and the above relation becomes the expression $\delta S/I = -2e^*$ in Eq. (1). In the presence of edge reconstruction, g becomes larger than ν . In Eq. (S20), we find the expression of $\delta S/I$ as a function of g (rather than as a function of κ) since g can be measured in experiments.

As shown in Eq. (S20), the excess noise δS is negative when $g < 1/2$. The negative excess noise is a signature of the fractional statistics of anyons propagating in the inner channels. In the opposite case of $g > 1/2$, δS is positive. For $\nu = 1/3$, the dependence of δS on g is drawn in Fig. S3(b). Note that the results are independent of the distance d between QPC1 and QPC2 on Edge2, unlike the case of an additional co-propagating outer edge channel discussed in the previous section. The independence is due to the fractionalization of a voltage-biased anyon into two counter-propagating parts on Edge2.

There have been experimental reports [14, 15] of observing $g < 1/2$ in a FQH system with filling factor $1/3$. The fact that g is observed to be larger than $1/3$ implies that there occurs edge reconstruction. In the cases of the reports of observing $g < 1/2$, we expect the possibility that one can observe the negative excess noise $\delta S < 0$, a signature of the fractional statistics.

* Corresponding author. hssim@kaist.ac.kr

- [1] J. von Delft and H. Schoeller, Bosonization for Beginners—Refermionization for Experts, *Ann. Phys. (Leipzig)* **7**, 225 (1998).
- [2] X. G. Wen, Chiral Luttinger liquid and the edge excitations in the fractional quantum Hall states, *Phys. Rev. B* **41**, 12838 (1990).
- [3] R. Guyon, P. Devillard, T. Martin, and I. Safi, Klein factors in multiple fractional quantum Hall edge tunneling, *Phys. Rev. B* **65**, 153304 (2002).
- [4] Chenjie Wang and D. E. Feldman, Fluctuation-dissipation theorem for chiral systems in nonequilibrium steady states, *Phys. Rev. B* **84**, 235315 (2011).
- [5] Chenjie Wang and D. E. Feldman, Chirality, Causality, and Fluctuation-Dissipation Theorems in Nonequilibrium Steady States, *Phys. Rev. Lett.* **110**, 030602 (2013).
- [6] O. Smits, J. K. Slingerland, and S. H. Simon, Non-equilibrium noise in the (non-)Abelian fractional quantum Hall effect, arxiv.org/pdf/1401.4581.
- [7] I. Safi, P. Devillard, and T. Martin, Partition noise and statistics in the fractional quantum Hall effect, *Phys. Rev. Lett.* **86**, 4628 (2001).
- [8] Eun-Ah Kim, Michael J. Lawler, Smitha Vishveshwara, and Eduardo Fradkin, Signatures of Fractional Statistics in Noise Experiments in Quantum Hall Fluids, *Phys. Rev. Lett.* **95**, 176402 (2005).
- [9] C. Han, J. Park, Y. Gefen, and H.-S. Sim, Topological vacuum bubbles by anyon braiding, *Nat. Commun.* **7**, 11131 (2016).
- [10] C. L. Kane and Matthew P. A. Fisher, Shot noise and the transmission of dilute Laughlin quasiparticles, *Phys. Rev. B* **67**, 045307 (2003).
- [11] Bernd Rosenow and Bertrand I. Halperin, Nonuniversal Behavior of Scattering between Fractional Quantum Hall Edges, *Phys. Rev. Lett.* **88**, 096404 (2002).
- [12] Sanghun An, P. Jiang, H. Choi, W. Kang, S. H. Simon, L. N. Pfeiffer, K. W. West, and K. W. Baldwin, Braiding of Abelian and Non-Abelian Anyons in the Fractional Quantum Hall Effect, [arXiv.org/abs/1112.3400](https://arxiv.org/abs/1112.3400) (2011).
- [13] S. Baer, C. Rössler, T. Ihn, K. Ensslin, C. Reichl, and W. Wegscheider, Experimental prove of topological orders and edge excitations in the second Landau Level, *Phys. Rev. B* **90**, 075403 (2014).
- [14] L. Saminadayar and D. C. Glatthli, Observation of the $e/3$ Fractionally Charged Laughlin Quasiparticle, *Phys. Rev. Lett.* **79**, 2526 (1997).
- [15] Stefano Roddaro, Vittorio Pellegrini, and Fabio Beltram, Nonlinear Quasiparticle Tunneling between Fractional Quantum Hall Edges, *Phys. Rev. Lett.* **90**, 046805 (2003).

- [16] R. Guyon, P. Devillard, T. Martin, and I. Safi, Klein factors in multiple fractional quantum hall edge tunneling, Phys. Rev. B **65**, 153304 (2014).